AIAA Guidance, Navigation, and Control Conference and Exhibit
1111 - 14 August 2003, Austin, Texas

AIAA 2003-5562

Gyro Modeling and Estimation of Its Random Noise Sources

Quang M. Lam, Nick Stamatakos, Craig Woodruff, and Sandy Ashton
Swales Aerospace
Guidance, Navigation, and control Group
5050 Powder Mill Road
Beltsville, MD 20705
www.swales.com

Abstract

The objective of this paper is twofold: (1) present a unit scaling based approach to model gyro random noise sources and (2) design and develop a ground-based software tool to extract the gyro random noise sources in terms of the statistical one sigma value of each noise source using both gyro rate and gyro angle data. The proposed approach is developed using two different techniques, Power Spectral Density (PSD) and Allan Variance. The proposed solution is implemented using Matlab/Simulink, and its performance is validated using high fidelity simulation data. Final tools will be designed for telemetry data processing in support of the GOES Program Office during the Post Launch Test (PLT) period. These tools will be used to characterize the on-orbit gyro noise performance and capture its state of health so that the GOES star tracker/gyro-based attitude determination system performance can be maintained or enhanced via the latest knowledge of gyro random noise sources.

Introduction

Gyro systematic errors due to biases, scale factors, and misalignments can be compensated for via an on-board Kalman filtering approach. On the other hand, gyro random noise sources -- such as angular white noise (AWN), angular random walk (ARW), and rate random walk (RRW) -- are not easily estimated by an on-board filter, due to their random characteristics. Ground-based software tools that are capable of estimating gyro random noise sources (i.e., AWN, ARW, and RRW) at any time after launch would be very useful to the maintenance and performance enhancement of the on-board attitude determination filter, since the filter performance is primarily dictated by the accuracy of the process noise covariance matrix, Q, that is a function of gyro random noise sources (see [6,7,8] &[12]).

Many times, random walk processes (i.e., RRW and ARW) are not modeled properly in the time domain to correctly capture the random walk nature, as intended by the IRU manufacturers. This modeling problem is due in large part to the peculiar units of $rad/sec^{1.5}$ and $rad/sec^{0.5}$ typically used for RRW and ARW, respectively. In order to truly match the gyro measurement at both rate and angle levels, a time scaling factor needs to be applied to these noise sources prior to integration for them to become true random walk processes. This scaling, many times in the past, has not been correctly applied (i.e., the incorrectly applied scaling factor typically reflects only straight time integration but not for unit consistency.) This paper presents a unit scaling based approach that properly produces the RRW and ARW noise sources which consistently match the units of the gyro rate and angle measurements.

A good knowledge of Gyro or Inertial Reference Unit (IRU) random noise sources is also important and critical to the overall space mission. IRU performance degradation due to aging or unexpected failures needs to be detected and corrected either autonomously, on-board or on the ground and then corrections sent via upload to the spacecraft to preserve mission life. In addition, a good knowledge of these noise sources and systematic errors after launch will also be beneficial to the performance enhancement of the attitude determination and control system during normal operation and orbit adjust mode. High rate and large angle slewing profiles utilized by special missions or during orbit adjust maneuvers demand even better knowledge accuracy of the IRU's "state of health."

This paper presents a practical approach to allow the engineer/scientist to properly capture the IRU performance characteristics at any time after launch in order to support and maintain mission operations. IRU or gyro performance parameters identified by the proposed system can be used to update the attitude determination filter process noise matrix in order to maintain its optimal performance.

Gyro Model Description

This section describes various gyro models employed in order to analyze the extraction of gyro noise error parameters. The complexity or fidelity of the gyro model necessary is dictated by the attitude determination design requirements. The primary reason for this discussion on various gyro models is to arrive at a generic model with adequate fidelity to mathematically capture the true dynamics of the gyro measurement throughout the dynamic range of the sensed rate (i.e., from low rate to high rate magnitude).

Depending on what the design objectives of the system are, the gyro model utilized may have different levels of fidelity (and sometimes these gyro models are not necessarily true representatives of the real-world gyro dynamics). For instance, the traditional six state attitude determination (AD) Kalman filter (e.g., see [1]) employs the following gyro model:

$$\omega_g = \omega + b + n_a \qquad (1)$$

where ω is the true rate, b is the gyro drift rate bias (rad/sec) driven by the RRW process (see Figure 1), and n_a is white noise corrupting the gyro rate measurement but becoming the angular random walk (rad/√sec) at the gyro angle level. Since the 6 state filter is intended to "extract" the gyro bias fluctuation under the formulation of equation (1), this gyro model is deemed adequate for this design objective.

Note that scale factor and misalignment errors are not accounted for in the model described in equation (1) since the 6 state AD filter is not designed to estimate those error parameters. Clearly there is no performance issue associated with such a gyro model (employed by the flight software side) for normal operations, i.e., nominal spacecraft rate vector in the orbit rate range. For missions that require high rate or large angle slew operations; however, a higher fidelity gyro model (e.g., see [2]) needs to be employed such as:

$$\omega_g = \omega + b + k_g + k_{ma} + n_a \qquad (2)$$

where k_g and k_{ma} are the gyro scale factor and misalignment errors, respectively, modeled as a function of true rates as described below:

$$\begin{bmatrix} k_{gx} \\ k_{gy} \\ k_{gz} \end{bmatrix} = \begin{bmatrix} g_{sfx} & 0 & 0 \\ 0 & g_{sfy} & 0 \\ 0 & 0 & g_{sfz} \end{bmatrix} \cdot \begin{bmatrix} \omega_x \\ \omega_y \\ \omega_z \end{bmatrix} \qquad (3)$$

$$\begin{bmatrix} k_{max} \\ k_{may} \\ k_{maz} \end{bmatrix} = \begin{bmatrix} 0 & g_{xy} & g_{xz} \\ g_{yx} & 0 & g_{yz} \\ g_{zx} & g_{zy} & 0 \end{bmatrix} \cdot \begin{bmatrix} \omega_x \\ \omega_y \\ \omega_z \end{bmatrix} \qquad (4)$$

Here g_{sfi} and g_{ij} (i and j represent the corresponding axis index) represent IRU vendor performance specifications in terms of parts per million (ppm) and thus are unitless

The total error due to scale factor and misalignment errors can be captured by a single equation:

$$\omega_{sfma} = G \cdot \omega \qquad (5)$$

where G is an augmented matrix of both the scale factor errors and misalignment errors described in equations (3) and (4):

$$G = \begin{bmatrix} g_{sfx} & g_{xy} & g_{xz} \\ g_{yx} & g_{sfy} & g_{yz} \\ g_{zx} & g_{zy} & g_{sfz} \end{bmatrix} \qquad (6)$$

Up to this point, the gyro measurement is still at the rate level. In reality, gyro measurement

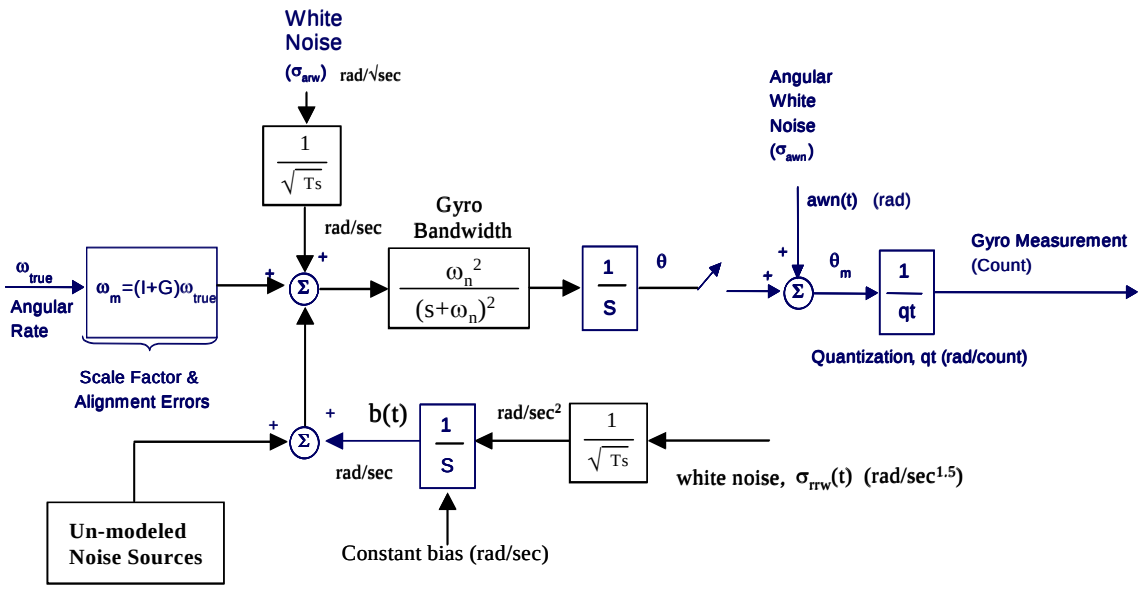

Figure 1: IRU Model

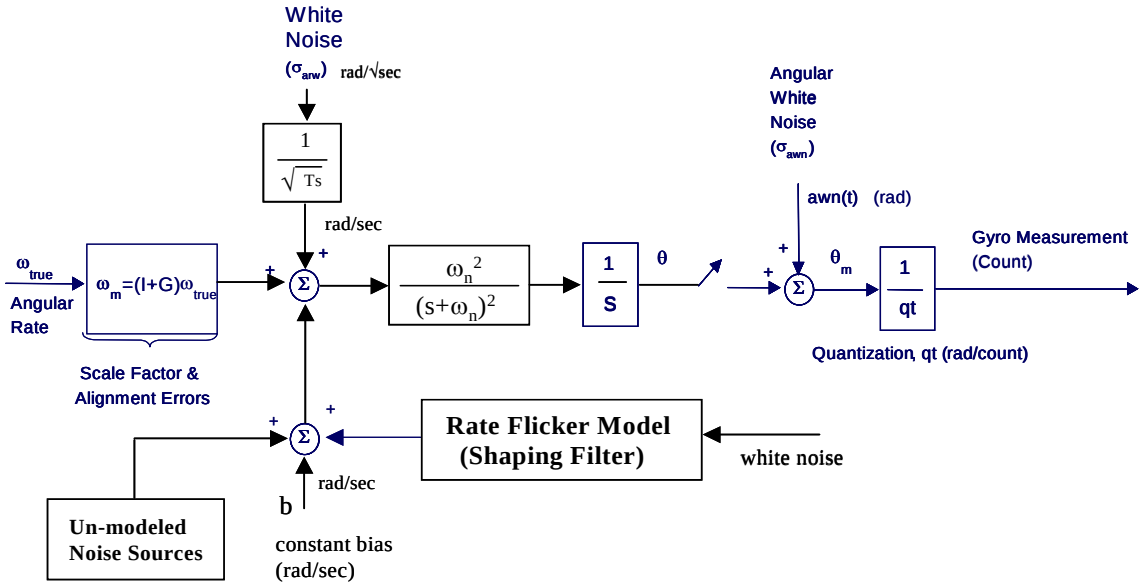

Figure 2: IRU Model With Rate Flicker Noise Model Replacing the RRW

output is available in either accumulated counts (angle) or delta counts (rate) depending on the manufacturer's design. Therefore, equation (2) needs to be integrated to produce gyro measured angles, and the electronic white noise (i.e., angular white noise) corrupting this angle measurement needs to be taken into account. Figure 1 illustrates the gyro model at both rate and angle levels with the actual gyro output being measured in counts that now accounts for the quantization error.

Note that the units of all gyro noise sources have been taken into account by "scaling" the IRU sampling time at the right junction of the RRW and ARW white noise generators. It is worth pointing out here that this modeling scheme has rarely been described at this detailed level elsewhere in the

literature. The model developed herein has been validated using Monte Carlo simulation with 400 runs to confirm the total drift error against the vendor specification.

The model described in Figure 1 is used to validate our gyro noise extraction and identification process. Note that for other types of IRUs, rate random walk can be modeled or captured by a different noise term, namely rate flicker noise. The "exchange roles" of rate random walk (RRW) and rate flicker (RF) noises are depicted in Figures 1 and 2. In general, rate flicker is a correlated noise process. The shaping filters shown in Figure 2 are determined by fitting low order filters to autocorrelation function or PSD curves. These curves are determined from real test data [10]

PSD Mathematical background and Noise Estimation Technique

The power spectral density (PSD) describes how the power or variance of a time series is distributed over a frequency range. Mathematically, it is defined as the Fourier Transform of the autocorrelation sequence of the time series. An equivalent definition of PSD is the squared modulus of the Fourier transform of the time series, scaled by a proper constant term. Typical units of PSD are rad^2/Hz for angle measurement signals, and $(rad/sec)^2/Hz$ for angular rate signals.

The gyro measurement contains a composite of AWN, ARW, and RRW; in order to individually extract the one-sigma value (1 σ) of each noise source utilizing the PSD output, specific post processing techniques need to be employed. This post-processing is accomplished by exploiting the unique characteristic of each noise source in the PSD data, as illustrated in Figures 3, 4, 5 and 6, respectively. For instance, AWN has zero slope, ARW has a slope of –2, and RRW has a slope of –4 in a log-log scale of angle PSD data. (See Table 1 for details.) Using these characteristics on the plot, individual noise source 1 σ value can be isolated and then extracted. Note, the term "angle PSD" refers to the PSD of an angular attitude signal (units of radians); whereas, "rate PSD" refers to the PSD of an angular rate signal (units of radians/second).

Figure 3 demonstrates that the mean of the angle PSD of AWN alone is a constant, i.e., the log-log slope is 0 (see [4], page 56). Figure 4 contains the curve of the angle PSD given ARW input, only – which is integrated white noise. The slope is constant on a log-log scale (see [4], page 56), and the slope should be close to -2. Figure 5 contains the curve of the angle PSD given RRW input only with a slope close to –4. Figure 6 is the angle PSD given all three-noise sources contained in one signal (the composite). At very low frequencies, the RRW dominates (10^{-4} to 10^{-3} Hz for this particular case); in the middle frequency range, the ARW is largest (10^{-2} to 10^{-2} Hz); and at the high frequencies the AWN dominates the response. In general, the relative positions of these effects on the PSD plot will not change. However, if and at what frequency range these effects become dominant depends on the input PSD level of the noise sources.

From the curve fits shown in Figure 6, one can estimate the input noise levels (either input PSD or variance). The procedure to obtain such an estimate is discussed below.

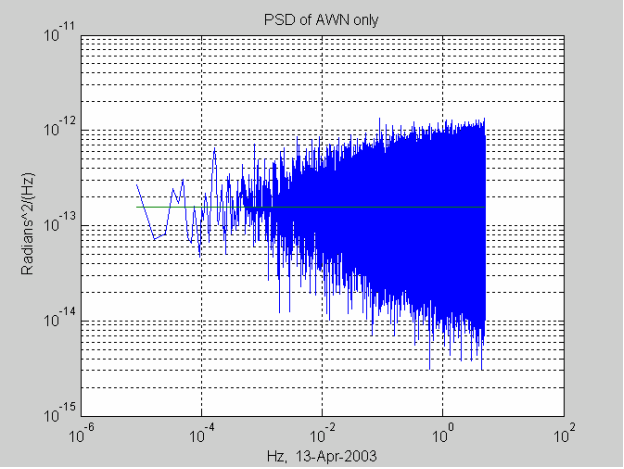

Figure 3: Angle PSD given AWN noise input only. (Blue curve is the PSD of angle; green curve is constant log-log fit; also, a low pass anti-aliasing filter, bandwidth of 10 Hz, was employed to reduce high frequency noise)

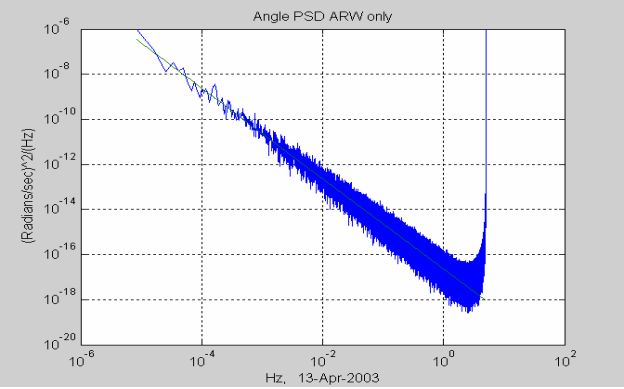

Figure 4: Angle PSD given ARW noise input only. (Blue curve is the PSD of angle; green curve is a least squares log-log fit; also, a low pass anti-aliasing filter, bandwidth of 40 Hz, was employed to reduce high frequency noise. Also, the "spike" occurring at high frequency is due to the use of the "twosided" PSD (pwelch) function in MATLAB. One-sided PSD (the default) does not produce this spike.)

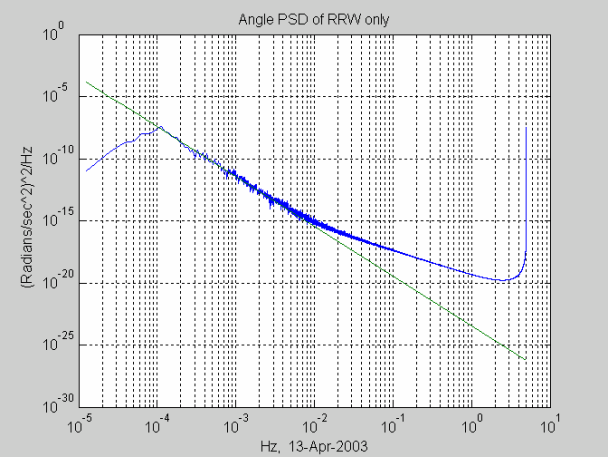

Figure 5: Angle PSD given RRW noise input only. (Blue curve is the PSD of the angle; green curve is a least squares log-log fit. Again, note that the "spike" occurring at high frequency is due to the use of the "twosided" PSD (pwelch) function in MATLAB. One-sided PSD (the default) does not produce this spike. Also, a high pass filter, bandwidth of 0.0001 Hz, was employed to, in-effect, detrend the data – which is required by the PSD (pwelch) command in MATLAB.)

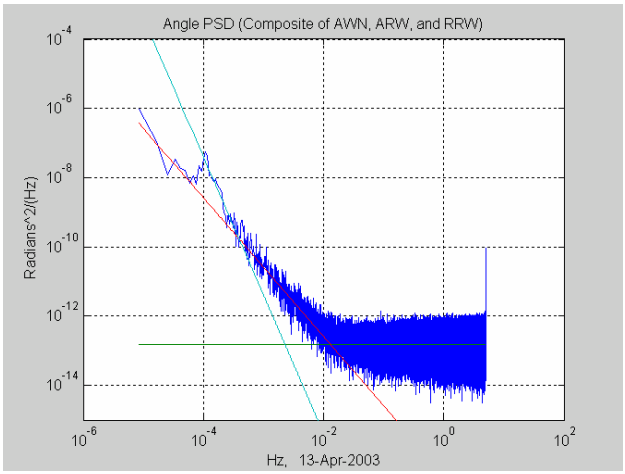

Figure 6: Angle PSD given AWN, ARW, and RRW noise input. (Blue curve is PSD of angle; green curve is constant log-log fit of AWN; and green and red curve are least-squares fits of ARW and RRW, respectively)

The first step is to compute the PSD of the total integrated rate error that includes all noise sources:

$$X_{Total\_noise} = PSD(\int(\omega_m - \hat{\omega})dt) \quad (7)$$

where ω_m is the gyro raw rate and $\hat{\omega}$ is the estimated rate available from the attitude determination system. Note that the estimated rate can be obtained via different sources. These include ephemeris data block or predicted model. The main objective is to remove the orbit rate from gyro random noise sources.

To separate the total noise into individual AWN, ARW, RRW noise sources, one must use the principle described in Table 1. Note that for angular random walk (i.e., integration of white noise) and rate random walk (i.e, double integration of white noise), the frequency $\omega=2\pi f$ has to be taken into account at a log-log scale of the PSD signal so that their 1 sigma values can be properly estimated using the "slope definition" described in Table 1.

In general, the PSD is calculated via the Fourier Transform of the autocorrelation (square power) of x(n). This relation is re-stated below:

$$X(e^{j\omega}) = \sum_{n=-\infty}^{+\infty} |x(n)|^2 e^{-j\omega n} \quad (8)$$

The AWN PSD input level estimate, isolated from the total PSD of all noise sources, X_{isol_AWN} , or the variance (1-sigma squared) can be obtained using the following equations:

$$X_{isol\_AWN} = X_{total\_noise}\left(f_{\text{i=1:n\_awn}}\right) \quad (9A)$$

where, $f_{\text{i=1:n\_awn}}$ are the frequencies at which the slope of the total PSD is close to 0.0.

$$\hat{\sigma}_{awn} = \sqrt{\frac{\sum_{i=1}^{n\_awn} X_{isol\_AWN}}{n\_awn - 1}} \quad (9B)$$

The quantity, $X_{\text{total\_noise}}$, is the PSD, at each frequency i of the total signal x(n). The "n_awn" in the summation in equation 9B, is the index of the frequency corresponding to the bandwidth of the noise process that is identified by the "zero slope", on a log-log scale, of the entire PSD (the zero slope of AWN can be seen Figures 3 or 6). (Equation (9B) can also be interpreted as the square-root of the average of the AWN portion of the total PSD of angle.)

The ARW PSD input level estimate, isolated from the total PSD of all noise sources, X_{isol_ARW} , can be obtained using the following equations:

$$X_{isol\_ARW} = \frac{X_{total\_noise}\left(f_{\text{i=1:n\_arw}}\right)}{\left(2\pi f_{\text{i=1:n\_arw}}\right)^2} \quad (10A)$$

where, $f_{\text{i=1:n\_arw}}$ are the frequencies at which the slope of the total PSD is close to -2.

$$\hat{\sigma}_{ARW} = \sqrt{\frac{\sum_{i=1}^{n\_arw} X_{isol\_ARW}}{n\_arw - 1}} \quad (10B)$$

The quantity, $X_{\text{isol\_ARW}}$, is the PSD, at each frequency i of the signal x(n). The "n_arw" in the summation in equation 10B, is the index of the frequency corresponding to the bandwidth of the gyro noise process that is identified by the "+2 slope", on a log-log scale, of the entire PSD. By examining equation 10A, one can calculate that the slope of the angle PSD plot to be –2, as was demonstrated in Figure 4.

The RRW PSD input level estimate, isolated from the total PSD of all noise sources, is obtained via a very similar process to that identified for the ARW above. However, the slope on the log-log angle PSD plot is identified as –4 for the RRW. The equations to identify the RRW variance are listed below and the procedure is the same as indicated for the ARW, substituting slope identification of –4 instead of –2.

$$X_{isol\_RRW} = \frac{X_{total\_noise}\left(f_{\text{i=1:n\_rrw}}\right)}{\left(2\pi f_{\text{i=1:n\_rrw}}\right)^4} \quad (11A)$$

where, $f_{\text{i=1:n\_rrw}}$ are the frequencies at which the slope of the total PSD is close to -4.

$$\hat{\sigma}_{RRW} = \sqrt{\frac{\sum_{i=1}^{n\_rrw} X_{isol\_RRW}}{n\_rrw - 1}} \quad (11B)$$

The ARW and the RRW are obtained by integrating their appropriate white noise processes, once for ARW and twice for RRW. One obtains the integral, in the frequency domain, -- of a noise signal represented in the time-domain by the following relation (for PSD's and FFT's):

$$X^2_{angle_i} = \frac{X^2_{rate_i}}{(2\pi f_i)^2} \quad (12)$$

One should note that the PSD relations in equations 10 and 11 obey the simple relation given in equation 12, as expected. These relations are summarized in the Table 1.

When one obtains test data that contains a composite of AWN, ARW, and RRW, clearly the

PSD presented in Figure 6 can be interpreted and post-processed as shown above. However, the PSD of flight telemetry from the gyros will contain a mode at orbit rate and harmonics. This rate must be removed from the PSD in order to effectively identify gyro random noise sources.

Figure 7 contains a PSD plot with the GEO orbit rate included to illustrate that the AWN, ARW, and RRW are totally masked by the orbit rate, for this case. Note that the GEO rate is relatively large (as compared to gyro random noise signatures) that the AWN, ARW, and RRW are completely masked. The GEO rate must be filtered out of the signal in order to proceed with gyro parameter noise estimation.

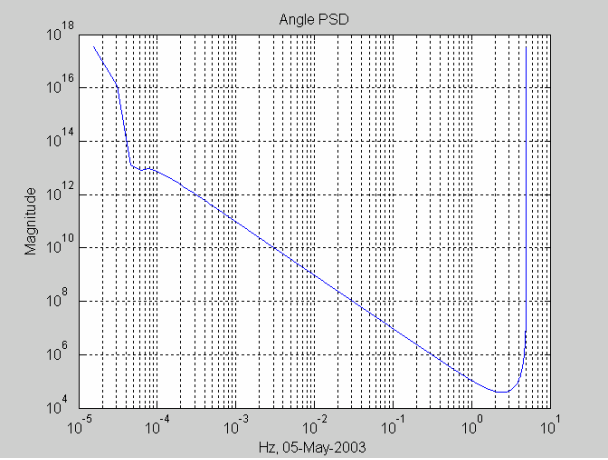

Figure 7: Angle PSD given GEO rate, AWN, ARW, and RRW noise input.

The post-processing techniques for final identification of the one-sigma values of these noise sources are summarized as follows:

AWN, ARW, and RRW Estimation Criterion: The output of the PSD performed on the gyro angles will have three portions: (1) Downward (negative) slope of –4, (2) downward slope of –2, and (3) horizontal slope of 0. The slope of –4 corresponds to RRW, slope of –2 to ARW, and slope of 0 to AWN. For this particular determination, analysts/engineers need to perform a manual judgment/analysis to properly isolate and identify the ARW from the AWN. In other words, formulas described in equation 7 through 12 and in Table 1 will be used for AWN, ARW, and RRW for the PSD or variance (one-sigma squared) estimation. The frequency intervals of the downward slope portion and the horizontal portion must be determined and entered by users. *Note that for random walk process, the one-sigma value calculation needs to be repeated for several sets of gyro data to more accurately finalize its estimated value.* The performance of the PSD approach described above will be summarized later and a comparison made with that of the Allan Variance approach.

Allan Variance Background and Technique

Computing the Allan variances is another powerful method for estimating the gyro random noise sources discussed to this point. In addition, other noise sources listed in reference 4 can also be evaluated with this technique.

The historical method of specifying drift or random error in terms of a single RMS number, even when associated with a correlation time, was inadequate for predicting system performance, leading to some very conservative means of specification. More recently, frequency domain methods proved superior for evaluating performance, but difficult for non-system analysts to understand. Also, frequency domain analysis techniques typically employ PSD calculations that require generally expensive software packages, such as MATLAB signal processing toolbox. The Allan variance is a method of representing RMS random drift or random error as a function of averaging time – which requires very little complicated mathematics or expensive software packages. [4]

The Allan variance, although computed using time averaging of time clusters, T, can also be related to the two-sided PSD, $S\Omega(f)$ by:

$$\sigma^2_{A,\Omega}(T) = 4\int_0^\infty S_\Omega(f)\frac{\sin^4 \pi fT}{(\pi f\tau)T}df \quad (13)$$

where, Ω is the gyro rate, and $S_\Omega(f)$ is the two-sided PSD.

Reference [4] contains an excellent summary table which lists 12 separate possible gyro noise sources and the corresponding angle and rate Allan variance plot and PSD characteristics. Also, that

table lists useful relationships of the rate or angle Allan variance ($\sigma_{A,\Omega}{}^2(T)$ and $\sigma_{A,\theta}{}^2(T)$, respectively) and input noise levels (e.g., σ^2_{ARW}, σ^2_{AWN}, and σ^2_{RRW}); and finally, it contains a composite, idealized, sample plot of Allan variance analysis results [4]. Table 2 summarizes the PSD and Allan variance slopes for some of the noise sources listed in [4]. Also, for several of these 12 individual noise sources, idealized Allan variance plots are made both in [4] and [3], to illustrate how each contributes to the composite plot.

Reference 5 also describes the estimation quality of Allan variances, which is useful when computing RRW, rate flicker, or rate ramp noise parameters. Typically, these noise sources are slowly varying phenomenon so the amount of data needed from gyro rate or angle measurements to determine the noise parameters is higher than for AWN and ARW. Thus, there is higher probability uncertainty in the determination of RRW, rate flicker, and rate ramp noise parameters than for AWN and ARW.

Similar to the previous section on PSD techniques, the Allan variance plots for each individual noise source are shown in Figures 8 through 10. In short, the Allan variance plot is computed by finding the statistical variance of cluster times, T_i, where i can vary from as 2 to n/2. The span of time covered by T_2 would be half the sample time, and $T_{n/2}$ would span just 2 samples. The Allan variance plot which contains the combined noise sources (the composite) is shown in Figure 11. Just as with the PSD composite plot, this Allan variance plot is what one would obtain from test data.

The post-processing techniques for final identification of the input PSD or one-sigma values of these noise sources from test data using Allan variances is very similar to that using the PSD technique discussed above. When analyzing flight data, the spacecraft orbit rate must be filtered out. for the ARW estimation. The PSD approach, however, must be used cautiously in estimating the As shown in Figure 12, below, the GEO orbit rate is large enough that the AWN, ARW, and RRW noise sources are totally swamped.

AWN, ARW, and RRW Estimation Criterion: The output of the Allan Standard Deviation performed on the gyro angles will have three portions: (1) Downward (negative) slope of –1/2, (2) upward (positive) slope of +1/2, and (3) upward slope of between +1 and +1_1/2. . The slope of –1/2 corresponds to AWN, slope of +1/2 to ARW, and slope of +1 to +1_1/2 to RRW. For this particular determination, analysts/engineers need to perform a manual judgment/analysis to properly isolate and identify the ARW from the AWN. In other words, formulas described in Table 1 will be used for AWN, ARW, and RRW for the input PSD or variance (one-sigma squared) estimation. The "time-cluster" intervals of the various portions of the curve must be determined and entered by the user.

The equations relating the Allan Variance to noise input PSD levels in Table 1 are obtained by analytically or numerically evaluating the integral equation 13 (above). It is worth noting that the input PSD level is a constant in equation 13, and the PSD is not evaluated for Allan Variance calculations. Although this integral is complicated, it needs to be evaluated only once for the AWN and ARW noise sources – and the results are listed for the reader in Table 1. The evaluation of the integral for the RRW is much more complicated; and numerical techniques were employed to estimate the integral.

Discussion and Summary

A performance comparison of PSD and Allan Variance approaches was conducted using simulated data and the results are shown in Table 2. Both approaches indicate promising results in reconstructing the one-sigma values of gyro random noise sources. The PSD approach (based on these sample cases) currently seems to be more accurate than that of the Allan Variance approach

Table 1: Estimated Gyro Random Noise Using PSD and Allan Variance Approaches

Noise source	PSD slopes: Angle, θ	PSD slopes: Rate, Ω	Estimated 1 sigma of Gyro Random Noise as a Function of Angle PSD	Allan Variance slopes: Angle, θ	Allan Variance slopes: Rate, Ω	Estimated 1 Sigma of Gyro Random Noise Using Allan Variance
White angle (AWN)	0	+2	$X_{isol\_ARW} = X_{total\_noise}\left(f_{i=1:n\_awn}\right)$ $\hat{\sigma}_{AWN} = \sqrt{\mu_{PSD,i=1:n\_awn}}$ μ_{PSD}=mean of gyro error angle PSD (defined in equation 8B)	-1/2	-1	$\sigma_{A,AWN,\theta}{}^2(T) = \frac{\sigma^2_{AWN,input}}{T}$ [3] $\hat{\sigma}_{AWN} = mean($ $10^{0.5*l10(T_i)+0.5*l10(\sigma_{A,AWN,\theta}{}^2(T_i))})$ where, l10 is log10 and $T_{i=1:n\_awn}$ are the time clusters whose slope is –1/2.
Angle Random Walk (ARW)	-2	0	$X_{isol\_ARW} = \frac{X_{total\_noise}\left(f_{i=1:n\_arw}\right)}{\left(2\pi f_{i=1:n\_arw}\right)^2}$ $\hat{\sigma}_{ARW} = \sqrt{\mu_{PSD,i=1:n\_arw}}$ where, $\mu_{PSD,i=1:n\_arw}$ is the mean of the log-log X_{isol_ARW}	+1/2	-1/2	$\sigma_{A,ARW,\theta}{}^2(T) = \frac{\sigma^2_{ARW,input}T}{3}$ $\hat{\sigma}_{ARW} = mean($ $10^{0.5*(l10(T_i)+l10(\sigma_{A,ARW,\theta}{}^2(T_i))+l10(3)}$) where, l10 is log10 and $T_{i=1:n\_arw}$ are the time clusters whose slope is +1/2.
Rate Flicker (RF)	-3	-1	$X_{isol\_RF} = \frac{X_{total\_noise}\left(f_{i=1:n\_rf}\right)}{\left(2\pi f_{i=1:n\_rf}\right)^3}$ $\hat{\sigma}_{RF} = \sqrt{\mu_{PSD,i=1:n\_rf}}$ where, $\mu_{PSD,i=1:n\_rf}$ is the mean of the log-log X_{isol_RF}	+1	0	$\sigma_{A,RF,\Omega}{}^2(T) \rightarrow \frac{2\sigma^2_{RF,input}\ln 2}{\pi}$ for T >> 1/ν, where 1/ν is the bandwidth of high pass filter.[2] Evaluation of $\hat{\sigma}_{RF}$ performed numerically.
Rate Random Walk (RRW)	-4	-2	$X_{isol\_RRW} = \frac{X_{total\_noise}\left(f_{i=1:n\_rrw}\right)}{\left(2\pi f_{i=1:n\_rrw}\right)^4}$ $\hat{\sigma}_{RRW} = \sqrt{\mu_{PSD,i=1:n\_rrw}}$ where, $\mu_{PSD,i=1:n\_rrw}$ is the mean of the log-log of $X_{isol\_RRW.}$	+1 ½	+1/2	$\sigma_{A,RRW,\Omega}{}^2(T) = \frac{\sigma^2_{RRW,input}T^2}{3}$ Evaluation of $\sigma_{A,RRW,\theta}{}^2(T)$ and $\hat{\sigma}_{RRW}$ performed numerically

[1] T is the cluster time associated with a cluster sample size M. M is defined in Figure 5, where N is the total number of samples broken into clusters of size M.

[2] Rate Flicker is often modeled as a "filtered" RRW or "pink noise".

[3] Note that the $\hat{\sigma}_{xxx}$ indicates an estimate using PSD or Allan variance processes; whereas, σ_{xxx} indicates an input white noise process. Also, $\sigma^2{}_{A,xxx}$ indicates an Allan Variance.

RRW because the PSD and FFT functions generally require detrending. Detrending of slowly varying processes must be done judiciously. Performance optimizations of these two approaches are currently being investigated.

Extensive simulated and real gyro test data as well as actual spacecraft telemetry data need to be used to fully validate the proposed estimation approaches.

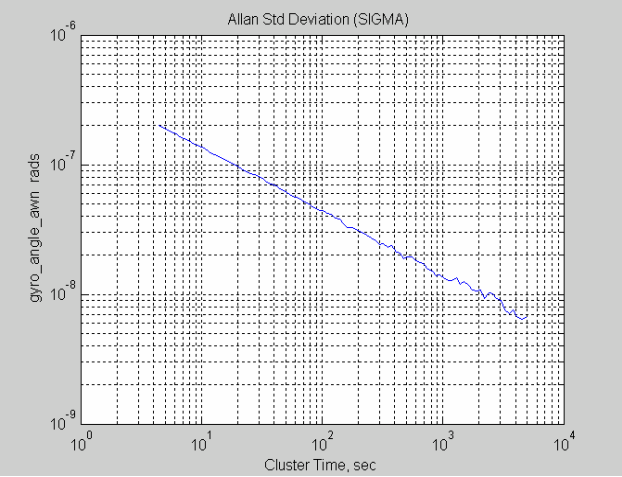

Figure 8: -- Allan Standard Deviation of Angle, $\sigma_{A,AWN,\theta}(T)$, given AWN Input only

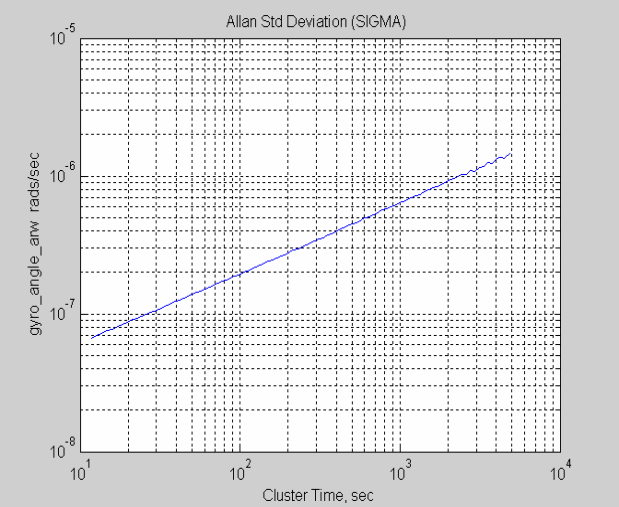

Figure 9: -- Allan Standard Deviation of Angle, $\sigma_{A,ARW,\theta}(T)$, given ARW Input only

A generic gyro model was developed to capture both systematic and random gyro error sources. Both PSD and Allan Variance approaches were examined in order to extract and identify gyro random noise sources. Current performance results indicate an encouraging direction in accurately estimating the one-sigma values of gyro random noise sources. The success of the proposed technique can be applied to enhance the performance of the on-board attitude determination filter by uploading these updated gyro random noise characteristics to the on-board filter process noise matrix. Future work will focus on signal separation design optimization, such as isolation of gyro noise sources from spacecraft body rate. This isolation design will clearly enhance the noise estimation accuracy since body dynamic and low frequency harmonics would not affect the PSD or Allan Variance calculation nearly as much. This will also help to capture the RRW term much more accurately, since now we can process data at longer duration without the body rate (and other low frequency terms) contaminating the RRW PSD average power.

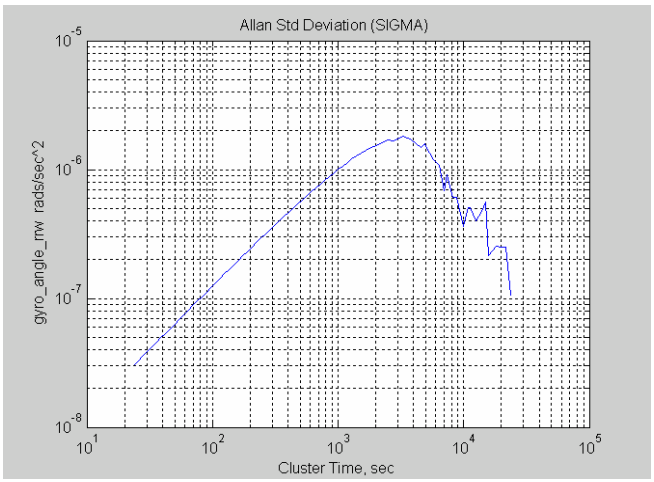

Figure 10: -- Allan Standard Deviation of Angle, $\sigma_{A,RRW,\theta}(T)$, given RRW Input only

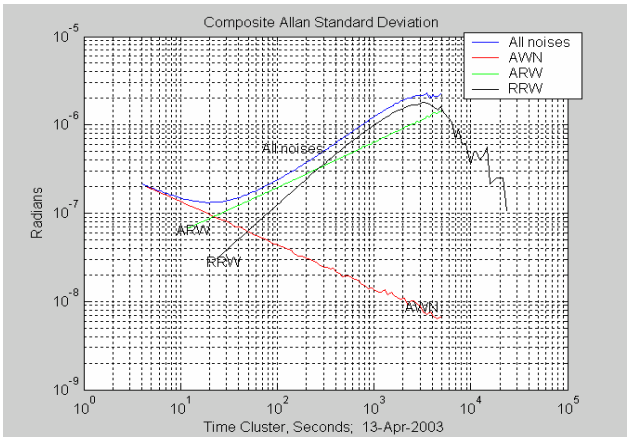

Figure 11: -- Composite Allan Standard Deviation on Angle, given combined ARW, AWN, and RRW Inputs

Table 2: Performance Summary

Gyro Random Noise Source	Truth Value	Identified Value (Allan Variance Approach)	Identified Value (PSD Approach)
Angular White Noise (rad/√Hz)	**4.36e-07**	**4.33e-07**	**4.33e-07**
Angular Random Walk (rad/√sec)	**3.35e-08**	**4.41e-08**	**3.23e-8**
Rate Random Walk (rad/sec$^{1.5}$)	**0.808e-12**	**1.16e-12**	**0.918e-12**
Flicker Rate Noise[1]	**3.00e-07**	**In Progress**	**In Progress**

[1] The Flicker Rate Noise is a "pink noise" process and the associated PSD and Allan Variance plots contain several slopes and "break-points"; thus, specifying single "unit" for this noise source is not possible

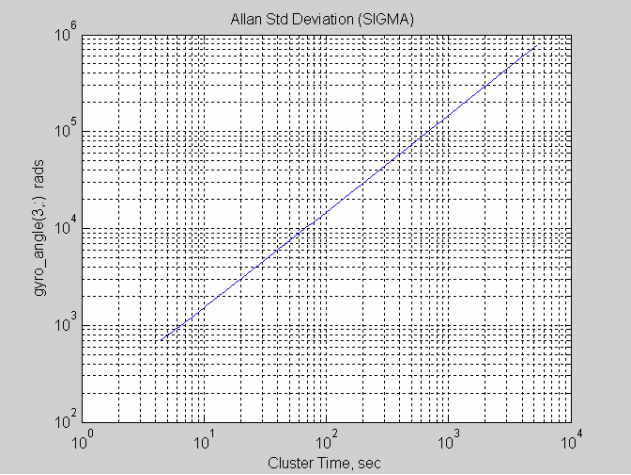

Figure 12: Angle Allan Variance given GEO rate, AWN, ARW, and RRW noise input. GEO rate must be filtered out of signal in order to proceed with gyro parameter noise estimation

Acknowledgements: The authors would like to thank Derrick Early and Jinho Kim for their helpful discussions and constructive inputs.

References

[1] Lefferts, E. J., Markley, F. L., and Shuster, M. D., Kalman Filtering for SpacecraftAttitude Estimation," AIAA Journal of Guidance, Control, and Dynamics, Vol. 5, No.5, 1982,

[2] Deutschmann, J. and Bar-Itzhack, I. Y., 'Extended Kalman Filter for Attitude Estimation of the Earth Radiation Budget Satellite," NASA CP-3050, Flight Mechanics and Estimation Theory Symposium, Greenbelt MD, May 10-11, 1989

[3] Ford, Jason; Evans, Michael, "Online Estimation of Allan Variance Parameters", Journal of Guidance, Control, and Dynamics, Vol. 23, No. 6, 12/2000.

[4] IEEE Standard Specification Format Guide and Test Procedure for Single-Axis Laser Gyros, IEEE Std 647-1995.

[5] Tehrani, M., M., "Ring Laser Gyro Data Analysis with Cluster Sampling Technique," Proceedings of the SPIE, vol. 412, 1983.

[6] Q. Lam, T. Hunt, P. Sanneman, and S. Underwood, " Analysis and Design of a Fifteen State Star Tracker/Gyro Based Filter Attitude Determination and Gyro Calibration System," AIAA GN&C Conference Paper 2003-5483.

[7] Pittelkau, M. E., "Kalman Filtering for Spacecraft System Alignment Calibration," AIAA Journal of Guidance, Control, and Dynamics, Vol. 24, No. 6, 2001

[8] Pittelkau, M. E., "An Analysis of the Quaternion Attitude Determination Filter," Paper AAS 03-194, Presented at the 2003 AAS/AIAA Space Flight Mechanics Conference, Ponce, Puerto Rico

[9] Papoulis, A., Probability, Random Variables, and Stochastic Processes," McGraw-Hill Book Company, 2nd Edition 1984, NY

[10] Grewal, Mohinder; and Andrews, Angus; Kalman Filtering: Theory and Practice Using MATLAB. 2nd Edition, John Wiley and Sons, Inc., 2001.

[11] Gradshteyn, I. S., Ryzhik, I. M.; "Table of Integrals, Series, and Products, 1980, Academic Press, New York.

[12] R. L. Farenkopf, "Generalized Results for Precision Attitude Reference Systems Using Gyros," AIAA Paper No. 74-903, AIAA Mechanics and Control of Flight Conference, August 5-9, 1974